



Global approach for the selection of high temperature comprehensive two-dimensional gas chromatography experimental conditions and quantitative analysis in regards to sulfur-containing compounds in heavy petroleum cuts

Laure Mahé^a, Thomas Dutriez^a, Marion Courtiade^{a,*}, Didier Thiébaud^b, Hugues Dulot^a, Fabrice Bertoncini^a

^a IFP Energies Nouvelles, Rond-point de l'échangeur de Solaize, BP 3, 69360 Solaize, France

^b LSABM, UMR CNRS 7195 PECSA, ESPCI, Laboratoire environnement et chimie analytique, 10 rue Vauquelin, 75231 Paris Cedex 05, France

ARTICLE INFO

Article history:

Received 11 October 2010

Received in revised form

24 November 2010

Accepted 26 November 2010

Available online 3 December 2010

Keywords:

1DGC

Selectivity

Enhanced elution

Vacuum gas oils

Petroleum

Ionic liquid columns

ABSTRACT

Extending the knowledge on sulfur-containing compounds is crucial for the petroleum industry because they contribute to atmospheric pollution by combustion. Most of them are concentrated in heavy petroleum cuts, such as vacuum gas oils (VGOs). However, the resolution of the existing analytical methods does not allow a quantitative speciation of S-compounds contained in VGOs. Therefore, a high temperature GC × GC chromatograph hyphenated to a SCD was implemented in this study to obtain a quantitative S-compounds speciation. Firstly, various thermally stable stationary phases, in particular the new ionic liquid IL59 and Mega Wax-HT, were investigated in 1D-GC as a way to reduce the number of columns sets to be used in GC × GC. Consequently, several normal and reversed configurations of these columns were selected and tested in GC × GC. Then, a decision method was applied to facilitate the choice of the best combination of columns. Finally, the most adapted methods led to an innovative group type quantification and to a quantitative distribution of heavy sulfur species contained in a VGO sample. These results represent a major step towards the study of S-compounds in heavy petroleum cuts.

© 2010 Elsevier B.V. All rights reserved.

1. Introduction

Sulfur is the principal heteroelement of crude oils. Despite its low content in light fractions, sulfur can represent up to 6 wt.% of the total elemental content in heavier ones. Sulfur-containing compounds include non-aromatic species (thiols, sulfides) and cyclic ones (thiophenes, benzothiophenes, dibenzothiophenes and homologues) [1]. They can induce air pollution as their combustion releases sulfur oxides (SO_x) in the atmosphere. Their presence in transportation oils and fluid catalytic cracking (FCC) feed is then continuously reduced by the legislation (10 ppm for gas oil in 2010 in the EU). Moreover, sulfur species promote corrosion in fuels [2] and reduce the efficiency of car catalytic converters by poisoning effect. In order to continuously improve hydrodesulfurization processes, including the selection of the most suitable catalysts, the kinetics of S-compounds behaviour at a molecular level [3] has to be well-known. Relationships between their molecular structures and their reactivities would give essential information on the cat-

alysts and process development, especially in regards to refractory compounds [4].

For a better understanding of S-compounds behaviour during conversion processes, an extended analytical characterization must be obtained on all kinds of petroleum samples. The molecular characterization of sulfur-containing compounds is easily performed on light cuts [5], e.g. gasolines, by gas chromatography hyphenated to a specific detector, flame photometric detector (pulseFPD), atomic emission detector (AED) or sulfur chemiluminescence detector (SCD). However, it remains difficult to deal with heavy petroleum cuts [6], in particular for a quantitative purpose [7]. Indeed, the complexity, i.e. the number of compounds, increases with the boiling point of the matrices, and only a S-compounds group type quantification is available for diesel and vacuum gas oil thanks to MS reference methods [8]. Moreover, S-compounds are especially concentrated in heavier cuts, which represent a continuously growing part of crude oils which are treated in refineries.

The implementation of comprehensive two-dimensional gas chromatographic techniques (GC × GC) [9,10] allowed a major breakthrough in the detailed characterization of organic-sulfur compounds contained in middle-distillates and heavy gas oils [11]. For instance, the hyphenation of GC × GC with a time-of-flight mass spectrometer [12,13] led to an efficient identification

* Corresponding author at: Physics and Analysis Division, IFP Energies Nouvelles, BP3, 69360 Solaize, France. Tel.: +33 04 37 70 20 76; fax: +33 04 37 70 27 45.

E-mail address: marion.courtiade@ifpenergiesnouvelles.fr (M. Courtiade).

of polyaromatic hydrocarbonated S-compounds (PAHS). Regarding the quantitative analysis of S-compounds contained in middle distillates, the hyphenation of a GC \times GC to various sulfur specific detectors (AED [14], SCD [15–17]) provided data by carbon atoms number and by group type, which is becoming a reference method [18]. However, GC \times GC is conventionally limited to the analysis of volatile compounds. Therefore ultra-mass spectrometric techniques, e.g. Fourier Transform Ion Cyclotron Resonance Mass Spectrometry (FT-ICR/MS) [19], have been implemented to a molecular analysis of heavy petroleum fractions. Extended knowledge in the identification of sulfur species [20] and in the understanding of hydrodesulfurization [21] have indeed been obtained thanks to this instrumentation. However, those results cannot be integrated in the process optimization steps, as quantitative results are not reachable yet.

Recently, high temperature GC \times GC (HT-2D-GC) allowed to open up new prospects on the extended quantitative characterization of heavy petroleum cuts [22,23]. Innovative results have already been obtained for hydrocarbons analysis [24], nitrogen-containing compounds characterization [25] and for the study of conversion processes [26,27] by tuning the GC \times GC system with extreme experimental conditions (i.e. very high modulation period and high temperature). The main limitation of HT-2D-GC is the thermal stability of polar stationary phases that induces a loss of selectivity at high temperature. Recent advances in terms of stationary phases chemistry offer some exciting possibilities for the development of new HT-GC \times GC methods. For instance, specific treatments of sol–gel phases [28] and GC stationary phases based on ionic liquids [29] have recently been introduced. In particular, the latter would give new selectivities [30] due to different solvation interactions. In addition, their low vapor pressures grant them high thermal stabilities [31]. Consequently, new possibilities have been reached out for the improvement of selectivity in GC \times GC [32,33] as well as for GC \times GC \times GC developments [34].

This study focuses on the development of a quantitative HT-2D-GC method in regards to the speciation of sulfur-containing compounds in heavy petroleum matrices. Therefore, the hyphenation of GC \times GC with an efficient SCD was performed. Several columns combinations, including the newly developed HT stationary phases, were investigated. The selection of adapted experimental conditions was obtained thanks to a global approach combining 1D-GC and GC \times GC experiments on test mixtures. Finally, a quantitative application on a vacuum gas oil will be shown.

2. Experimental

2.1. Samples and chemicals

Three standard mixtures were prepared using commercially available sulfur compounds, which are representative of the compounds contained in VGO samples and obtained from Chiron (Norway), Sigma–Aldrich (Lyon, France) and Pr. J. Andersson (University of Munster, Munster, Germany).

The first test mixture (TM1) was prepared in toluene and contained four sulfur compounds (compounds labeled 2, 7, 9 and 11 in Table 1). The second test mixture (TM2) was prepared in toluene using 13 sulfur compounds (Table 1) representative of compounds supposed to be contained in VGO samples. The third test mixture (TM3) contained three S-compounds belonging to various group types: C₁₆-thiophene, C₂₀-benzothiophene, C₂-dibenzothiophene (compounds labeled 1, 5 and 6 in Table 1). This test mixture was prepared in toluene at five different concentrations (0.1 ppm w/w S, 0.2 ppm w/w S, 0.3 ppm w/w S, 0.4 ppm w/w S and 0.5 ppm w/w S).

One vacuum gas oil was supplied by IFP Energies Nouvelles Lyon (Table 2). It comes from a mixture of several straight-run vacuum gas oils. Before the analysis, it was diluted in toluene (100 ppm of total sulfur content).

2.2. GC-SCD

All 1D experiments were conducted on a HP 6890 gas chromatograph (Agilent Technologies, Massy, France) hyphenated to a sulfur chemiluminescence detector (SCD) (355 Dual Plasma, Sievers, Agilent Technologies, Massy, France) and equipped with an on-column injector. A constant flow rate of helium (99.99% Air Liquide, France) close to the optimum velocity of the column was used as the carrier gas.

GC-SCD experiments were performed to study the selectivity of various stationary phases, i.e. capillary columns (Table 3), with S-compounds contained in test mixture 1. Experiments were carried out at isothermal conditions for four different temperatures: 175 °C, 200 °C, 225 °C and 250 °C.

2.3. GC \times GC-SCD experiments

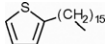
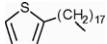
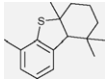
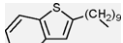
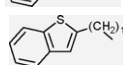
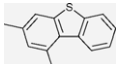
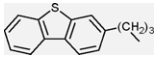
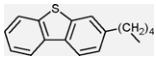
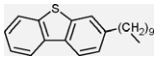
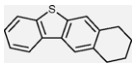
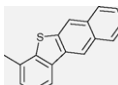
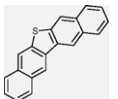
All 2D experiments were carried out using an in-house modified HP 6890 GC (Agilent Technologies, Massy, France) hyphenated to a sulfur chemiluminescence detector (SCD) (355 Dual Plasma, Sievers Boulder, CO, USA), equipped with a CO₂ dual jets modulator and an on-column injector. A constant flow rate of helium (99.99% Air Liquide, France) close to the optimum velocity of the first column was used as the carrier gas. The most suitable experimental conditions were determined by comparing different columns sets by GC \times GC. Their properties as well as the experimental conditions are compiled in Table 4. The length of the second column and the 2D modulation which was set at 20 s were longer than those of usual methods as elution temperatures of the first column were reduced. Hence, the inner diameter of the wide-bore first column was 0.25 mm or 0.32 mm in order to fulfill the Murphy bidimensional criterion [35,36] of 3 or 4 modulations per peak. The first dimension peak widths were indeed higher than 60 s in our experiments.

The acquisition rate of the SCD was set at 50 Hz. High sampling rate is indeed necessary to define properly the second dimension narrow peaks. Ruiz-Guerrero et al. [18] showed strong tailing of peaks with a SCD used in GC \times GC conditions. However, this lack of efficiency seems to correspond to the detection cell void volume. SCD is therefore compatible with GC \times GC experiments [18]. Moreover, in our experiments, the second dimension peak widths are quite large therefore a high acquisition rate of the SCD is less crucial. Raw data of SCD were acquired using the HP Chemstation software (Agilent) and exported as a CSV-file for GC \times GC data processing. GC \times GC contour plotting, retention time measurement, blob fitting and peak integration were performed using 2D Chrom™ (Thermo, Italy). Intensities are displayed via contrasting colors, ranging from pale blue to dark blue that represent, respectively, minor and major peaks.

2.4. GC \times GC-TOF/MS with offline LC fractionation

A LC fractionation between polycyclic aromatic hydrocarbons (PAHs) and polycyclic aromatic sulfur heterocycles (PASHs) was carried out on the VGO sample prior to the GC \times GC-TOF/MS analysis in order to simplify the analytical matrix. Ligand exchange chromatography was performed with a Pd-ACDA-silica column, which allows a separation between PAHs and PASHs [37–40]. This Pd column (150 mm \times 4 mm based on 10 μ m silica 100A pore size) was obtained from Pr. J. Andersson (University of Munster, Munster, Germany). The separation

Table 1
Composition of the test mixture 2.

Thiophenes					
1	Hexadecylthiophene (C ₁₆ -T)	C ₂₀ H ₃₆ S			
2	Octadecylthiophene (C ₁₈ -T)	C ₂₂ H ₄₀ S			
Naphtheno-thiophenes					
3	Me ₄ H ₆ Dibenzothiophene	C ₁₆ H ₂₂ S			
Benzothiophenes					
4	2-Decylbenzothiophene (C ₁₀ -BT)	C ₁₈ H ₂₈ S			
5	2-Eicosylbenzothiophene (C ₂₀ -BT)	C ₂₈ H ₄₆ S			
Dibenzothiophenes					
6	4,6-Dimethyldibenzothiophene (C ₂ -DBT)	C ₁₄ H ₁₂ S			
7	Butyldibenzothiophene (C ₄ -DBT)	C ₁₆ H ₁₆ S			
8	Pentyldibenzothiophene (C ₅ -DBT)	C ₁₇ H ₁₈ S			
9	4-Decyldibenzothiophene (C ₁₀ -DBT)	C ₂₂ H ₂₈ S			
Naphtheno-dibenzothiophenes					
10	Tetrahydronaphthothiophene	C ₁₆ H ₁₄ S			
Naphtodibenzothiophenes					
11	Naphtodibenzothiophene (C ₀ -NDBT)	C ₁₆ H ₁₀ S			
12	Methylnaphtodibenzothiophene (C ₁ -NDBT)	C ₁₇ H ₁₂ S			
Dinaphtodibenzothiophenes					
13	Dinaphtothiophene	C ₂₀ H ₁₂ S			

was conducted on an Alliance Waters HPLC system equipped with a diode array detector set between 220 and 300 nm (chromatogram extracted at 236 nm). PAHs compounds were eluted with a mixture of cyclohexane:dichloromethane (7:3 wt.) whereas PASHs compounds were eluted after the addition of isopropanol to the previous mobile phase up to 1 wt.%. The flow rate was set at 1 mL/min and the injection volume was 20 μ L.

Table 2
Physical characteristics and elementary composition of the VGO studied.

Sample	Density at 15 °C (g/cm ³) ^a	Total sulfur (%S) ^b	Total nitrogen (ppm N) ^c	Basic nitrogen (ppm N) ^d	Boiling point interval (°C) ^e
VGO	0.9237	2.41	836	235	366–533

^a Determined by NF ISO12185.

^b Determined by NF ISO14596 or ISO20884.

^c Determined by NF 07058 or ASTM D4629.

^d Determined by ATSM D-4729-03.

^e Determined by SimDist (ASTM D-2887) (5–95% weight).

GC \times GC-TOF/MS analysis was used to confirm the 2D elution zones previously determined thanks to the use of TM3. It consists in a 6890N (Agilent Technologies, Massy, France) gas chromatograph hyphenated to a Pegasus IV time-of-flight mass spectrometer (LECO, St. Joseph, MI, USA) and equipped with a liquid nitrogen modulator. Electron ionization was performed at 70 eV, the acquisition frequency was set at 100 Hz in a mass ranging from 50 to 600 amu and a multi-plate voltage of –1450 V was applied.

Table 3
Capillary columns properties for GC-SCD analyses.

Capillary column	Composition	Properties
BPX-50 ^a	50% Phenylpolysilphenylene-siloxane	3 m × 0.1 mm × 0.1 μm
DB1-HT ^b	100% Dimethylpolysiloxane	3 m × 0.1 mm × 0.1 μm
Mega Wax-HT ^c	Polyethylene glycol	3 m × 0.1 mm × 0.1 μm
IL59 ^d	Dicationic ionic liquid	3 m × 0.1 mm × 0.08 μm
DB5-HT ^b	5% Phenyl 95% dimethylpolysiloxane	30 m × 0.32 mm × 0.1 μm

^a SGE, Courtaboeuf, France.^b Agilent, Massy, France.^c Mega, Milan, Italy.^d Supelco, Saint-Quentin Fallavier, France.

ChromaTOF (LECO) software was used for the control of the chromatograph and of the detector, for the data collection and for data processing. Identification was performed by comparing the acquired mass spectrum with the NIST 2.0 (2002) mass spectra database or by spectral deconvolutions based on typical *m/z* fragments.

3. Results and discussion

High temperature conditions are required in order to analyze high boiling point compounds by gas chromatography (GC or GC × GC). The choice of HT columns is limited, especially polar ones, even though some new thermally stable stationary phases have recently been developed. Therefore, the first step of our study was to select a range of stationary phases (Table 3), from non polar to polar ones, which can be suitable for the GC × GC analysis of S-compounds at high temperature. This includes the new ionic liquid IL-59 and Mega Wax-HT (polyethylene glycol). Experiments were carried out by following a global approach, which will be explained later on, and by always keeping in mind the difficult equilibrium between the loss of elution at high temperatures and the desired high separation efficiency [22].

3.1. Setting of 2D conditions

The choice of a GC × GC columns set by monitoring 2D separation criteria is not always an easy task, as some results can be contradictory. A columns set can indeed display a good 2D resolution and a low 2D occupation. In fact, 2D separation exhibits a high

number of parameters which are interconnected [41]. Therefore, it is helpful to develop a methodology that will facilitate the choice of the best columns combination for a type of analysis. Firstly, conventional 1D-GC was implemented in order to conclude on the selectivity of sulfur-containing compounds towards selected stationary phases. This methodology will allow to gain time as each column is studied only in one dimension and to save consumables (cryogenic fluid) as there is no need to use 2D modulation. Secondly, interesting sets of columns were studied by GC × GC and 2D separation criteria were monitored. Those criteria will be brought together in a single decision factor that will allow the choice of the best column set. This two-step methodology will be followed in this study.

3.1.1. Comparison of capillary columns by GC-SCD

The enthalpy of interaction of compounds with a stationary phase can be evaluated using the Van't Hoff equation (Eq. (1)) [42] where *k* is the retention factor, Δ*H* is the enthalpy, *R* is the ideal gas constant, *T* is the temperature, Δ*S* is the entropy and φ is the phase ratio. In order to compare various stationary phases, ln(*k*) can be plotted against 1/*T*. This is called a Van't Hoff plot. However, this comparison can be done only if each column possesses the same phase ratio (which means the volume of the stationary phase divided by the volume of the mobile phase) and if the phase ratio of each column is constant over the analysis [42].

$$\ln(k) = \frac{\Delta H}{RT} + \frac{\Delta S}{R} + \ln(\varphi) \quad (1)$$

In order to remove the dependence between the compound retention time and the volume to phase ratio, columns were compared to each other via selectivity plots (that is plotting selectivity α as a function of 1/*T*) [33]. Indeed, the ratio between the retention factor of each compound represents the selectivity between both compounds, which removes the influence of the phase ratio when comparing each column.

All single dimension data were collected isothermally at four different temperatures: 175 °C, 200 °C, 225 °C and 250 °C. Each compound of TM1 was carefully chosen in order to conclude easily on its inter (by aromaticity) and intra (by alkylation) family interactions with each capillary column tested. In fact, information about interfamily interactions was acquired by comparing the selectivity between C₁₈-T and C₁₀-DBT as well as between C₄-DBT and C₀-NDBT with each capillary column. It is important to notice that each compared compound possesses the same number of carbon atoms. Concerning intrafamily interactions, information was obtained by comparing the selectivity between C₄-DBT and C₁₀-DBT with each capillary column.

Table 4
Experimental conditions for GC × GC-SCD analyses (see Table 3 for stationary phase composition).

Set	Configuration	First column	Second column	Oven temperature	
A	Normal	DB5-HT	BPX-50	100–370 °C/2 °C/min	
B		30 m × 0.32 mm × 0.1 μm	1.2 m × 0.1 mm × 0.1 μm		
C		DB5-HT	Mega Wax-HT		
D		30 m × 0.32 mm × 0.1 μm	70 cm × 0.1 mm × 0.1 μm		
E	Reversed	DB5-HT	IL59	100–300 °C/2 °C/min	
F		30 m × 0.32 mm × 0.1 μm	1 m × 0.1 mm × 0.1 μm		
G		BPX-50	IL59		
H		20 m × 0.25 mm × 0.1 μm	1.5 m × 0.1 mm × 0.1 μm		
A		IL59	DB1-HT		100–300 °C/2 °C/min
B		10 m × 0.25 mm × 0.2 μm	80 cm × 0.1 mm × 0.1 μm		
C		IL59	DB5-HT		
D		10 m × 0.25 mm × 0.2 μm	70 cm × 0.1 mm × 0.1 μm		
E	Reversed	IL59	BPX-50	100–300 °C/2 °C/min	
F		10 m × 0.25 mm × 0.2 μm	50 cm × 0.1 mm × 0.1 μm		
G		BPX-50	DB5-HT		
H		20 m × 0.25 mm × 0.1 μm	3 m × 0.1 mm × 0.1 μm		

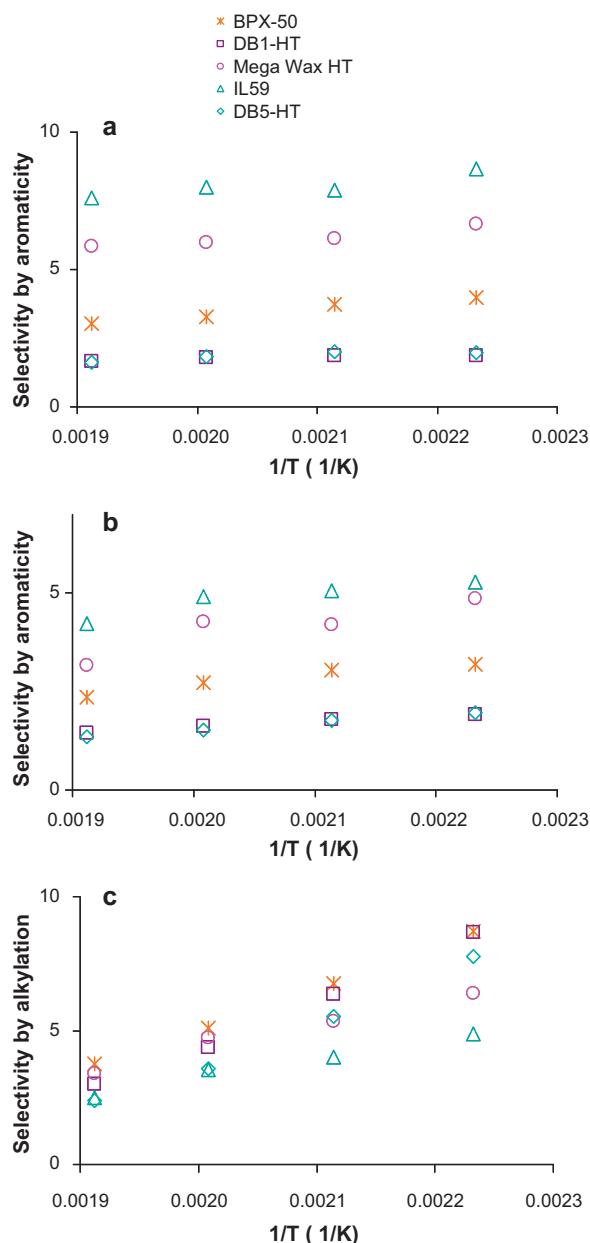


Fig. 1. Selectivity plots (a) interfamily interaction between C18-T and C10-DBT, (b) interfamily interaction between C4-DBT and C0-NDBT, (c) intrafamily interaction between C4-DBT and C10-DBT. * : BPX-50, □ : DB1-HT, ○ : Mega Wax HT, △ : IL-59, ◇ : DB5-HT. See conditions in Section 2.2.

The selectivity plots illustrating each type of interactions for each column are shown in Fig. 1. We can conclude that IL59 and Mega Wax-HT are much more selective towards highly aromatic sulfur-containing compounds than BPX-50, DB1-HT and DB5-HT. Thus, they will act as polar columns towards this family of compounds. On the other hand, BPX-50, DB1-HT and DB5-HT are more selective towards compounds with a high alkylation degree than IL59 and Mega Wax-HT. Hence, they will exhibit the same properties as non-polar columns. In conclusion, in normal configuration (also called orthogonal), BPX-50, DB1-HT and DB5-HT should be used as first column and IL59 and Mega wax-HT as second column. In a reversed configuration (also called non-orthogonal), the contrary should be done in order to obtain the best separation of S-compounds contained in VGO samples.

3.1.2. Comparison of capillary columns by GC × GC-SCD

Based on the observation made thanks to conventional 1D-GC, eight different sets of columns were chosen in order to confirm our assumptions (Table 4). The geometry of columns was selected to give a similar spread of solutes in the 2D contour plots. Therefore, the length of the first column was chosen in order to scatter the model compounds in the first dimension scale. In addition, the length of the second column was adjusted to obtain similar space occupations of peaks in the second dimension. Thus, 2D contour plots of the test mixture 2 obtained via these sets are given in Fig. 2: four normal configurations (A, B, C and D) and four reversed configurations (E, F, G and H). Firstly, some qualitative information can be observed. In normal configuration, set A is the only one that possesses elution bands parallel to the first dimension. This means that characterization of heavy sulfur compounds will be more accurate with set A than with sets B, C and D. Set D is interesting indeed as a reversed configuration could be expected based on the polarity of the first column (i.e. towards π - π interactions). In fact, it can be concluded that IL59 is more selective than BPX-50 towards cyclic S-compounds. This provides information about the behaviour of IL59 which is consistent with the results obtained in conventional 1D-GC. In reversed configuration, sets E, F and G provide a good spreading of solutes. In fact, with these three sets, a better separation between chemical families is achieved, especially towards naphtheno-aromatic compounds. The first conclusion is that a better separation by carbon atoms number is expected with a normal configuration whereas with a reversed configuration a better separation by group type is likely to happen, especially for less aromatic compounds. Peaks in sets D and H are wide in both dimensions, which indicates low efficiencies. Thus, many coelutions are expected when analysing VGO samples with those two columns sets. Except for sets D and H, it is still hard to choose the best combination of columns based only on qualitative comments. Thus, bidimensional separation criteria are required in order to quantify the performances of each 2D system and to confirm first qualitative observations.

3.1.3. Monitoring of bidimensional separation criteria

In order to evaluate and compare the performances of each investigated 2D system, bidimensional separation criteria were used [43].

RS_{2D} between solutes A and B is defined by Giddings [9] as the Euclidian norm of the resolution over the two axes Eq. (2).

$$RS_{2D} = \sqrt{{}^1RS^2 + {}^2RS^2} \quad (2)$$

The 2D resolution was calculated via Eq. (3), where ω is the peak width along each dimension and Δtr is the difference of retention between the apexes of the two compounds. Peak widths were measured at 4σ in both dimensions. Peak widths (${}^1\omega$) in the first dimension are considered to be equal to the product of the number of modulations by the modulation period.

$$RS_{2D} = \sqrt{\frac{2(\Delta {}^1tr)^2}{({}^1\omega_A + {}^1\omega_B)^2} + \frac{2(\Delta {}^2tr)^2}{({}^2\omega_A + {}^2\omega_B)^2}} \quad (3)$$

In this study, the interfamily resolutions were obtained by calculating 2D resolutions between C₁₆-T and C₁₀-BT, C₁₀-BT and C₄-DBT as well as between tetrahydro-NDBT and C₀-NDBT as they were close in the 2D contour plots (Fig. 3a). The intrafamily 2D resolutions were reached out by evaluating the 2D resolutions between C₄-DBT and C₅-DBT as well as between C₀-NDBT and C₁-NDBT as they were close in the 2D contour plots (Fig. 3b). Based on 1D-GC convention, RS_{2D} is sufficient when it is higher than 1.5. It is clear that sets E, F and G exhibit the best 2D resolutions by group type while set H exhibits the worst one. Differences between 2D

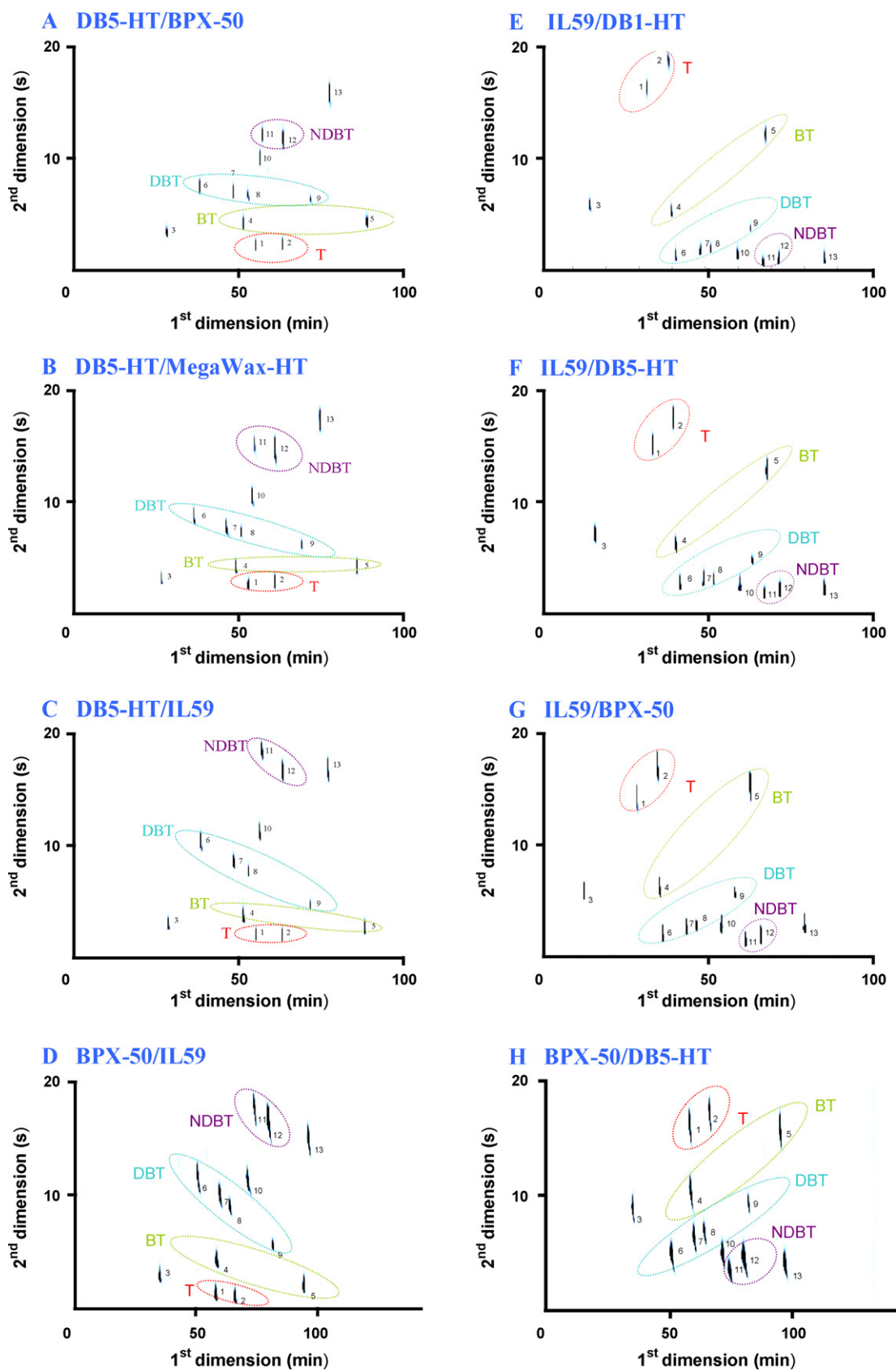


Fig. 2. 2D contour plots of TM2 (see Table 1) for 8 different experimental conditions (see conditions in Section 2.3). T: thiophenes; BT: benzothiophenes; DBT: dibenzothiophenes; NDBT: naphthodibenzothiophenes; DNDBT: naphthodibenzothiophenes.

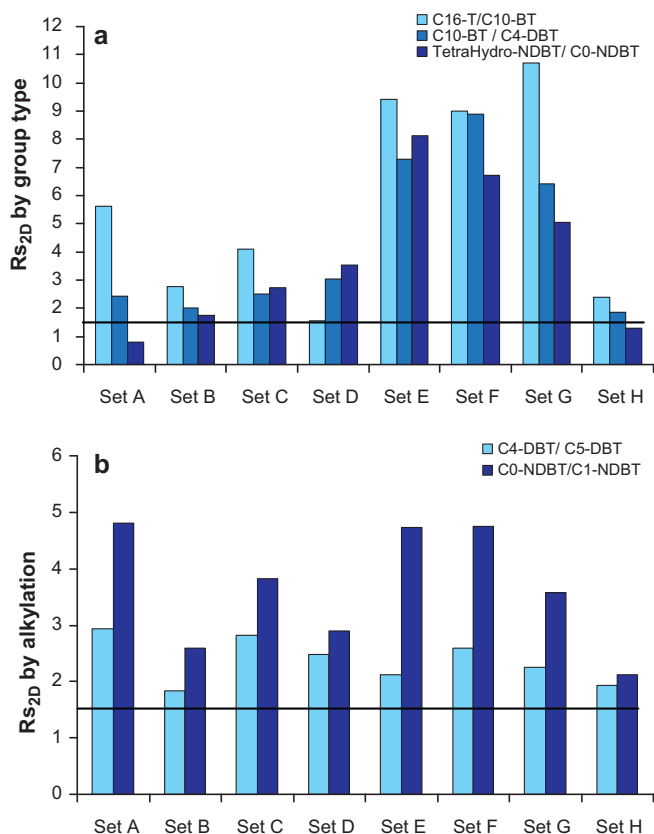


Fig. 3. Comparison of 2D resolutions (a) by group type and (b) by alkylation for selected peaks in TM2 2D contour plots of the eight column sets.

resolutions by alkylation are less significant.

Peak shape can be altered by several chromatographic conditions and a resulting unsymmetrical peak is usually observed for heavy compounds in GC × GC analysis. Dutriez et al. [22], recently introduced 2D asymmetry (As_{2D}) based on geometrical considerations where the apex of the overall peak is considered to be the apex of the most intense slice and where dimensionless values represent the distance between the apex and the extremities of the peak. The As_{2D} was calculated using Eq. (4) to compare the results obtained with the eight experimental conditions: ${}^1\omega$ and ${}^2\omega$ correspond to peak widths at 13%, respectively, in the first dimension and in the second dimension (for the most intense slice).

$$As_{2D} = \frac{\sqrt{(\Delta^2 tr_f / {}^2\omega)^2 + (\Delta^1 tr_b / {}^1\omega)^2}}{\sqrt{(\Delta^2 tr_b / {}^2\omega)^2 + (\Delta^1 tr_f / {}^1\omega)^2}} \quad (4)$$

Five compounds (labeled 1, 5, 8, 11 and 13) of each aromatic class were used in this calculation. The best 2D asymmetries are obtained when results are close to 1. Compared to the other, columns sets D, E, F exhibit the best overall 2D asymmetries (Fig. 4a).

The concept of 2D peak capacity production, recently employed by Siegler et al. [34], was chosen in order to estimate the efficiency of the 2D systems to separate a high number of solutes. 2D capacity production was then calculated using Eq. (5) where $n_{c,2D}$ is the peak capacity of the system, 1t_r is the running time, P_{mod} is the 2D modulation period, ${}^1\omega$ and ${}^2\omega$ are, respectively, the peak widths at 13% in the first and second dimensions. 2D capacity production was calculated on the same peaks as 2D asymmetry.

$$\frac{n_{c,2D}}{{}^1t_r} = \frac{P_{mod}}{{}^1\omega} \times \frac{1}{{}^2\omega} \quad (5)$$

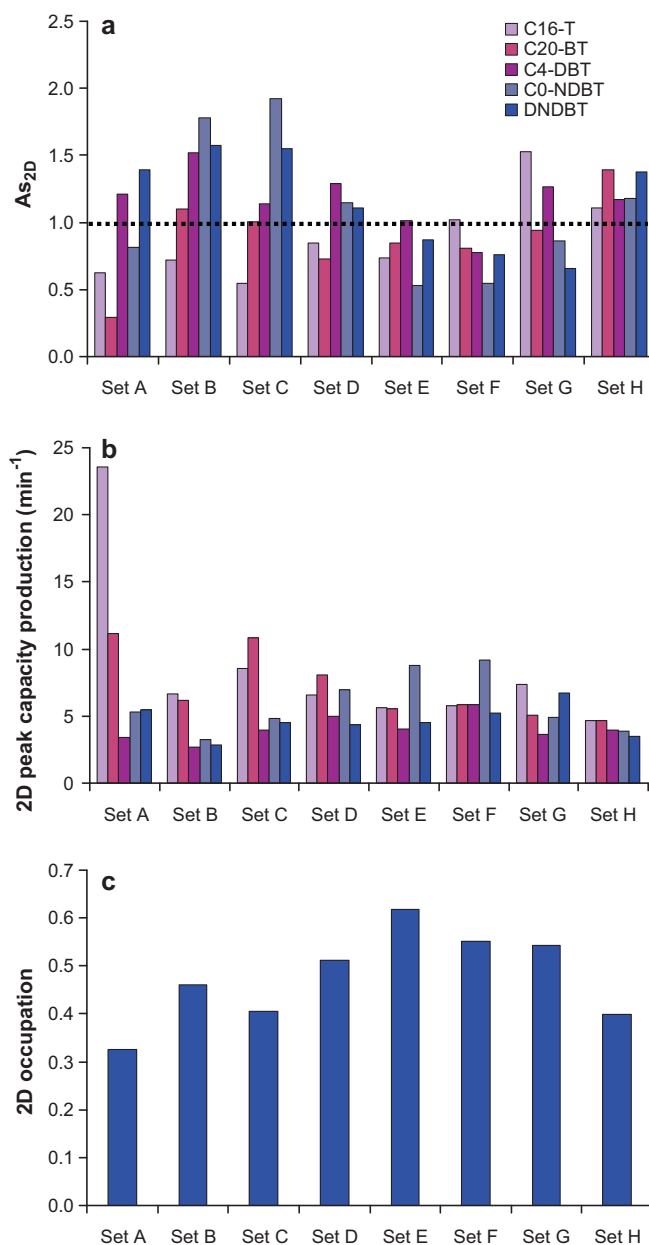


Fig. 4. Comparison of (a) 2D asymmetries, (b) 2D peak capacity production and (c) 2D occupation for selected peaks in TM2 2D contour plots of the eight columns sets.

It is quite hard to determine which columns set exhibits the best 2D peak capacity production as it really depends on the 2D elution zone of the peak of interest. Indeed, in Fig. 4b, set A displays the best capacity production calculated for C16-T but also one of the worst one for C4-DBT. It is then quite difficult to choose the best set considering only this bidimensional separation criterion. However, it is important to notice that highly aromatic compounds exhibit the best 2D peak capacity production in reversed configuration. On the contrary, slightly aromatic compounds, like thiophenes or benzothiophenes, provide the best 2D peak capacity production in normal configuration. This observation is consistent with the time spent by each compound in the second dimension. In fact, highly aromatic compounds elute later on a reversed configuration (that is to say a polar column in the first dimension), which increases the 2D peak capacity production.

2D occupation was calculated in order to quantify the spreading of peaks in 2D contour plots [25,44]. The first and the last eluted

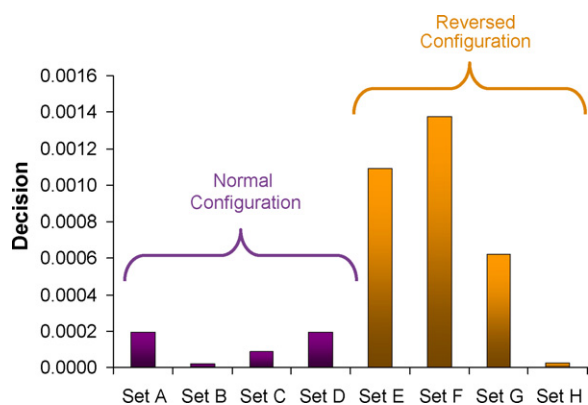


Fig. 5. Decision values for the eight column sets applied on the TM2.

peaks in each dimension were considered. It was calculated as shown in Eq. (6) where 1tr_a is the retention time of the first eluted peak in the first dimension, 1tr_b is the retention time of the last eluted peak in the first dimension, 2tr_c is the retention time of the first eluted peak in the second dimension, 2tr_d is the retention time of the last eluted peak in the second dimension, 1Tr is the run time and P_{mod} is the 2D modulation period.

$$2D \text{ Occupation} = \frac{^1tr_a - ^1tr_b}{^1Tr} \times \frac{^2tr_c - ^2tr_d}{P_{mod}} \quad (6)$$

In Fig. 4c, it is clear that sets E, F and G (reversed configuration) provide the best 2D occupation while sets of columns used in normal configuration exhibit the worst ones. This observation can be attributed to a lower selectivity by group type in normal configuration than in reversed configuration. It was indeed noticed in Section 3.1.2 that a reversed configuration was even able to separate naphtheno-aromatic sulfur containing compounds.

3.1.4. Choice of adapted 2D configurations

Those numerous results are difficult to interpret as they can exhibit contradictory effects on 2D separation performances [41]. Thus, adapted GC × GC-SCD experimental conditions were chosen using desirability functions [45–47]. This approach allows values whose responses are different to be converted into the same scale, based on desired behaviours, and also to be combined in order to provide an overall quality index representing the multiple parameters. Briefly, the value of each individual parameter is converted into a dimensionless number or 'desirability value' within 0 and 1, where 0 corresponds to a completely unacceptable value and 1 corresponds to a value which totally fulfills the requirements. Desirability functions were created by taking into account the optimum conditions of each response. An overall desirability (Decision) is then obtained by multiplying the individual desirability values or 'desirabilities' obtained for each parameter (Eq. (7)) [22].

$$\text{Decision} = \left(\prod_{i=1}^6 d_i \right)^{\frac{1}{2}} \quad (7)$$

In this study, individual desirability factors were calculated for each 2D separation criteria calculated in the previous part. This was done by considering linear functions for 2D resolutions, 2D peak capacity productions and 2D occupations and a polynomial function for 2D asymmetries. The decision factor for each column is shown in Fig. 5. In normal configuration, set A is the best combination whereas in reversed configuration set F is the best one. In comparison with the results obtained in 1D experiments, it is obvious that our first predictions are confirmed. Indeed, in regards to selectivity, DB5-HT was one of the best to separate compounds by alkylation, while IL59 was the best one to separate compounds

Table 5

Quantification limit of test mixture 3 determined by GC × GC-SCD analysis (set F). LQ: Quantification limit.

Compounds	LQ (ppm S)
C16-T	0.080
C2-DBT	0.024
C20-BT	0.038

by sulfur group type. As far as BPX-50 is concerned, this column exhibited a good selectivity towards highly aromatic and alkylated compounds. Thus, it can be assumed that the columns choices can be simplified by comparing their selectivities towards a family of compounds by conventional GC. However, GC × GC experiments are necessary in order to confirm the best columns set and to adapt columns lengths. In fact, 1D experiments help reducing the number of columns sets to be investigated in GC × GC.

3.2. Analysis of a VGO sample

3.2.1. Qualitative analysis

In order to confirm the 2D elution zones previously identified thanks to TM2, a GC × GC-TOF/MS analysis was carried out for set F by performing spectrum deconvolutions of the total ion current 2D contour plot. Prior to the analysis, the VGO matrix was separated into PAHs and PASHs fractions thanks to an offline separation by ligand exchange chromatography (see Section 2.4). Fig. 6 shows three selected ion fragmentation chromatograms of the VGO sample analyzed under set F experimental conditions using specific masses 161, 212 and 262, respectively, representative of benzothiophenes, dibenzothiophenes and naphthodibenzothiophenes chemical families. A clear distinction by carbon atoms number is reached out as well as a roof tile effect. The identification of isomeric compounds was not performed as our aim was to link a carbon atoms number to a group type. These results are consistent with the 2D elution zones identified via test mixture 2.

The VGO sample was analyzed using set A (normal configuration) and set F (reversed configuration) by GC × GC-SCD. Beforehand, the VGO was spiked with a reference compound (Me_4H_6 Dibenzothiophene labeled 9 in Table 1) in order to identify precisely the 2D elution zones in each VGO sample.

Fig. 7 shows the VGO sample analyzed via both sets A and F experimental conditions. The 2D elution zones were determined as described above. On the one hand, it is noticeable that a better spread by chemical groups is available with set F than with set A. This observation is in agreement with the one made with the test mixture experiments. The column bleeding seems to occur earlier for set F owing to the lower thermal stability of the columns than the ones of set A. This induces a loss of elution for highly aromatic compounds, what can prevent an accurate quantification of DNDBT family solutes. On the other hand, set A provides a better distinction by carbon atoms number.

3.2.2. Quantitative analysis

3.2.2.1. Analytical performances of the chromatographic system. The sensitivity and the equimolarity of the SCD were checked on TM3 for set F. The sensitivity was evaluated via the calculation of the detection limit (DIN 32645); it was found to be lower than 0.5 pg/s as specified by Agilent Technologies. Concentration was also plotted as a function of the peak height in order to obtain a quantification limit related to the concentration of sulfur atom. Each investigated compound had a limit of quantification lower than 0.8 ppb w/w of sulfur (Table 5). Thus, the SCD provides a very sensitive response for each sulfur-containing compound. The plot that displays the concentration as a function of the peak area shows three straight lines with a correlation coefficient higher than 0.9985

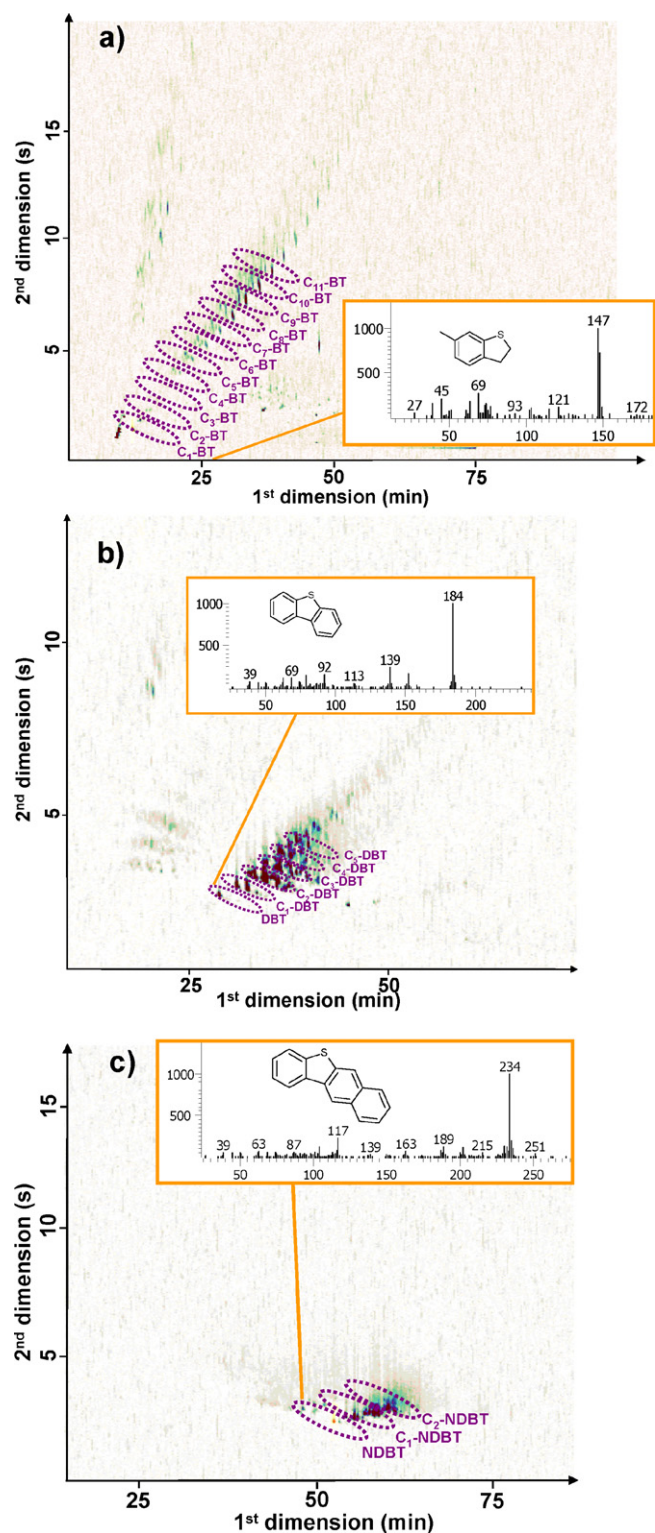


Fig. 6. GC \times GC-TOF/MS (a) ion fragmentation 161 specific of benzothiophenes (BT) derivatives, (b) ion fragmentation 212 specific of dibenzothiophenes (DBT) derivatives, (c) ion fragmentation 262 specific of naphthodibenzothiophenes (NDBT) derivatives. See conditions in Section 2.4.

for the selected compounds; their superimposition is obtained with a bias lower than 2% relative. It can then be concluded that the SCD gives an equimolar response for the investigated high boiling point sulfur-containing compounds. The equimolarity and the sensitivity of the detector allowed quantitative analysis to be performed on the VGO sample.

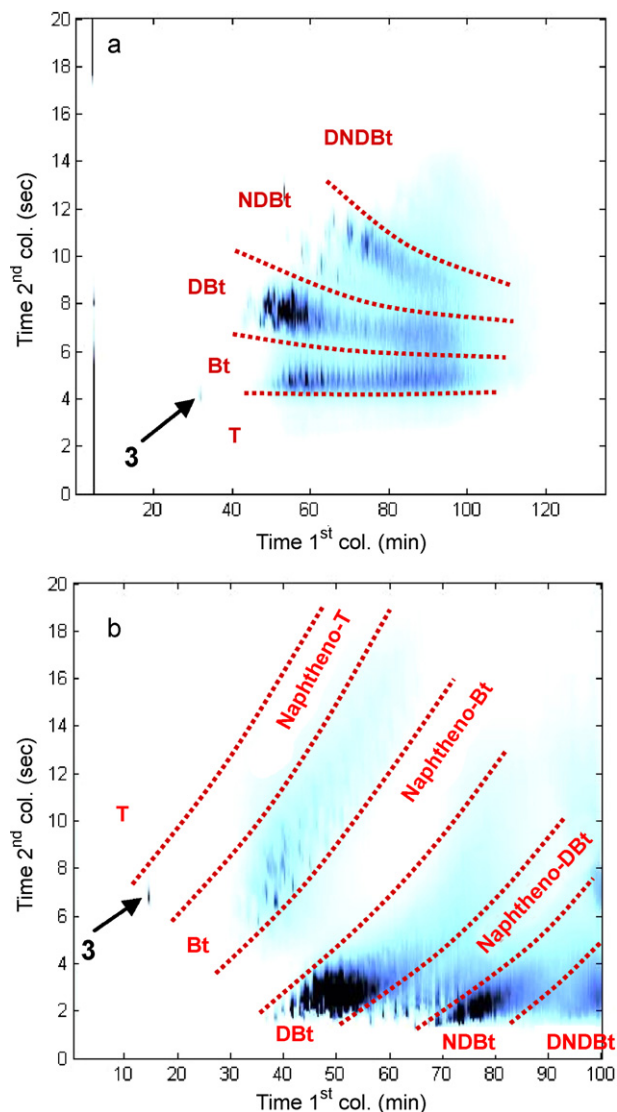


Fig. 7. 2D contour plots of a straight-run VGO using (a) set A and (b) set F. T: thiophenes, Bt: benzothiophenes, DBt: dibenzothiophenes, NDBt: naphthodibenzothiophenes, DNDBt: dinaphthodibenzothiophenes. See conditions in Section 2.3.

3.2.2.2. Quantification by group type. The quantification purpose was achieved by normalization to 100% of the 2D contour plots full area, as acceptable confidence intervals (four replicates) were calculated for each family and did not exceed 20%. Then, the concentration of each 2D elution area, e.g. sulfur group type, was corrected thanks to the total sulfur content determined by XRF reference method (NF ISO 14596 or ISO 20884).

Fig. 8 reveals the concentration (ppm S) of each sulfur compounds family contained in the VGO sample analyzed with by set A and set F experimental conditions. An extended group type quantification was achieved via set F, thanks to a better separation by naphtheno-aromatic sulfur compounds obtained with a reversed configuration than with a normal configuration. However, quantification results seem to be slightly biased owing to the lack of DNDBt elution. It appears that sulfur atoms are more concentrated in dibenzothiophenic structures in the VGO sample than in thiophenic compounds, which is consistent with the literature.

3.2.2.3. Quantification by carbon atoms number. To go further into the speciation of sulfur-containing compounds, a quantification by carbon atoms number was performed. Contrary to middle-

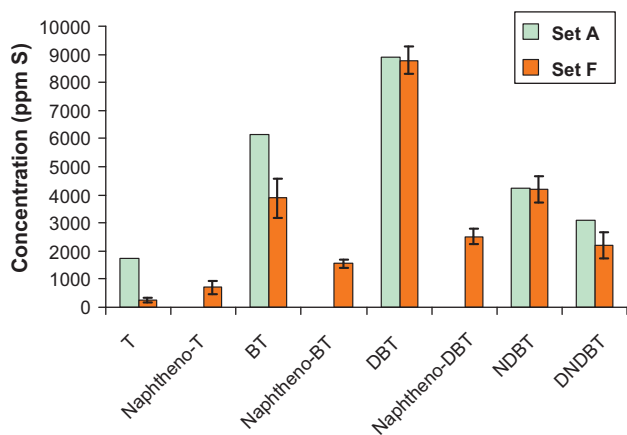


Fig. 8. Group type quantification for sulfur-containing compounds contained in the straight run VGO. T: thiophenes, BT: benzothiophenes, DBT: dibenzothiophenes, NDBT: naphthodibenzothiophenes, DNDBT: dinaphthodibenzothiophenes.

distillates samples, a complete distinction by carbon atoms number remains a daunting task to achieve on VGO samples. Actually, the elution bands that were almost parallel to the first dimension with set A facilitate this calculation. It is easier to calculate the equivalent carbon atoms number with this set as it only depends on the first dimension retention times. In fact, in reversed configuration (set F), carbon atoms number depends on both the first and the second dimension retention times which make the calculation more complicated. Therefore, group contribution methods [24] can be easily implemented on a 2D contour plot in order to obtain the equivalent carbon atoms number for each 2D elution zone with set A. Retention times of each modulated slice of sulfur group type in set A were then converted into a carbon atoms number. Moreover, it is important to notice that normal configurations gave a more detailed quantification by carbon atoms number for most of the aromatic S-compounds than reversed configurations.

Subsequently, the group type quantification obtained via set F was combined to the carbon atoms number quantification resulting from set A in order to obtain a concentration by carbon atoms number for each chemical family identified via set F. The correspondence between group types was done by considering each aromatic chemical class, including naphtheno-aromatic structures. The chemical formula, the molecular mass and the sulfur ratio of each S-compound were available from these results and allowed the conversion of concentrations by ppm S into weight percentages. The results are compiled in Fig. 9. The global bimodal curve obtained is consistent with the nature of the VGO analyzed (mixture of several VGOs).

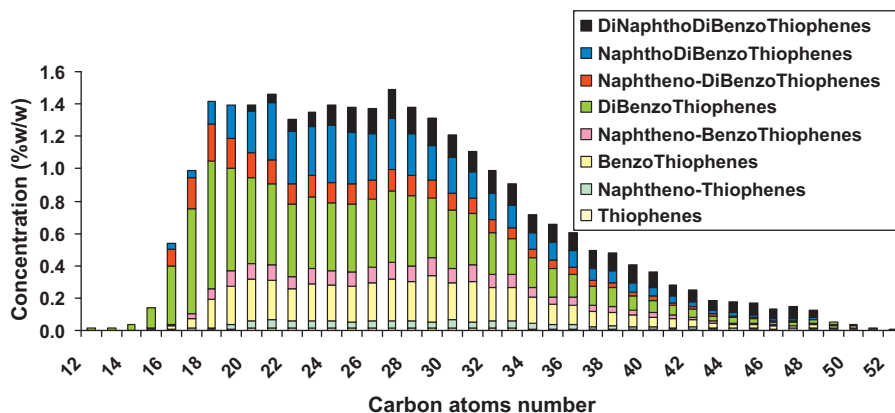


Fig. 9. Group type quantification by carbon atoms number for sulfur compounds contained in the VGO.

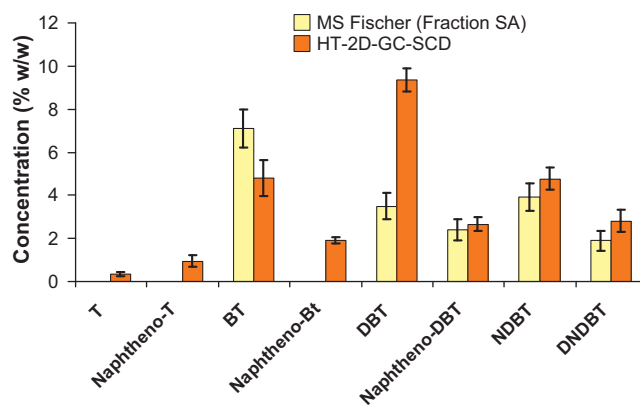


Fig. 10. Concentration (% w/w) of sulfur chemical families contained in the VGO by HT-2D-GC and MS Fischer method. T: thiophenes, BT: benzothiophenes, DBT: dibenzothiophenes, NDBT: naphthodibenzothiophenes, DNDBT: dinaphthodibenzothiophenes. SA: saturated and aromatic fractions.

Finally, the weight concentration of all sulfur-containing compounds inside the VGO (which means compared to the weight concentration of hydrocarbons, nitrogen compounds, . . .) can then be estimated. In this VGO, 27.5 wt.% of the VGO sample belongs to sulfur-containing compounds. The data overestimates the one obtained with MS Fischer method (18.8%) [48]. While good correlations between GC × GC-SCD and MS Fischer were obtained on diesel and straight run samples analysis [18]. This supports the evidence that the results obtained by MS Fischer underestimate the amount of sulfur containing compounds in VGOs since the resin fraction is removed beforehand. However, MS Fischer method does not take into account resins fraction and the assignment of m/z fragment can be biased by interferences [8]. The comparison of the quantification results obtained by HT-2D-GC-SCD and by MS Fischer method is provided in Fig. 10.

Extended group type quantification is achieved by HT-2D-GC-SCD on thiophenes and naphtheno-benzothiophenes when comparing with the data obtained with MS Fischer method. An overall agreement is observed for almost all families, except for the dibenzothiophenic one. This suggests that this S-compounds family is more concentrated in resins fraction than the others ones. Actually, this is quite in disagreement with the common knowledge on this polar fraction. Definitely, further experiments should be investigated to increase the knowledge on the structural composition about resins fractions. These results represent a major breakthrough for the study of heavy petroleum samples. It can indeed be helpful for further catalysts and processing improvements, in particular by kinetic modelling, as molar fractions are

now reachable for each sulfur chemical families contained in VGO samples [3].

4. Conclusion

The hyphenation of a HT-2D-GC to a specific SCD was presented in this study. The most thermally resistant stationary phases were studied including an ionic liquid phase. A pre-selection of the most suitable stationary phases was performed thanks to isothermal 1D experiments. Then, the comparison of selected column sets was carried out by GC × GC in normal and in reversed configurations. A statistical method allowed the gathering of 2D separation criteria and was implemented in order to choose the most adapted experimental conditions. Finally, a reversed mode using IL59 provided an innovative sulfur group type separation, especially for naphthoaromatic S-compounds family. Ground-breaking quantitative results were gained on a vacuum gas oil sample. The combination of those results with the ones from the normal configuration set allowed to reach out a carbon atoms number distribution. By this way, a deeper characterization of S-compounds was available. This work opens up new prospects for a better understanding of heavy sulfur-containing compounds behaviour during hydrodesulfurization process.

Acknowledgments

The authors wish to thank Pr. J. Andersson from University of Munster for the Pd-ACDA-silica column.

References

- [1] I. Merdrignac, D. Espinat, *Oil Gas Sci. Technol.* 62 (2007) 7.
- [2] M.C. Loeffler, N.C. Li, *Fuel* 64 (1985) 1047.
- [3] N. Charon-Revellin, H. Dulot, C. Lopez-Garcia, J. Jose, *Oil Gas Sci Technol.* (2010) In press.
- [4] T.R. Ling, B.Z. Wan, H.P. Lin, C.Y. Mou, *Ind. Eng. Chem. Res.* 48 (2009) 1797.
- [5] I.C. Lee, H.C. Ubanylonwu, *Fuel* 87 (2008) 312.
- [6] H. Behbehani, M.K. Andari, *Pet. Sci. Technol.* 18 (2000) 51.
- [7] F. Jimenez, V. Kafarov, A. Nunez, *Chem. Eng. J.* 134 (2007) 200.
- [8] A. Fafet, J. Bonnard, F. Prigent, *Oil Gas Sci. Technol.* 54 (1999) 453.
- [9] J.C. Giddings, *J. High Resolut. Chromatogr.* 10 (1987) 319.
- [10] H.J. Cortes, B. Winniford, J. Luong, M. Pursch, *J. Sep. Sci.* 32 (2009) 883.
- [11] T.V. Choudhary, *Ind. Eng. Chem. Res.* 46 (2007) 8363.
- [12] M. van Deursen, J. Beens, J. Reijenga, P. Lipman, C. Cramers, *J. High Resolut. Chromatogr.* 23 (2000) 507.
- [13] J. Dalluge, J. Beens, U.A.Th. Brinkman, *J. Chromatogr. A* 1000 (2003) 69.
- [14] L.L.R. van Stee, J. Beens, R.J.J. Vreuls, U.A.Th. Brinkman, *J. Chromatogr. A* 1019 (2003) 89.
- [15] W.F.C.-Y. Wang, *J. Sep. Sci.* 27 (2004) 468.
- [16] R. Hua, J. Wang, H. Kong, J. Liu, X. Lu, G. Xu, *J. Sep. Sci.* 27 (2004) 691.
- [17] J. Blomberg, T. Riemersma, M.v. Zuijlen, H. Chaabani, *J. Chromatogr. A* 1050 (2004) 77.
- [18] R. Ruiz-Guerrero, C. Vendeuvre, D. Thiebaut, F. Bertoncini, D. Espinat, *J. Chromatogr. Sci.* 44 (2006) 566.
- [19] L.A. Stanford, S. Kim, R.P. Rodgers, A.G. Marshall, *Energy Fuels* 20 (2006) 1664.
- [20] S.K. Panda, W. Schrader, J.T. Andersson, *Anal. Bioanal. Chem.* 392 (2008) 839.
- [21] A.A. Al-Hajji, H. Muller, O.R. Koseoglu, *Oil Gas Sci. Technol.* 63 (2008) 115.
- [22] T. Dutriez, M. Courtiade, D. Thiebaut, H. Dulot, F. Bertoncini, J. Vial, M.C. Hennion, *J. Chromatogr. A* 1216 (2009) 2905.
- [23] F. Bertoncini, F. Adam, T. Dutriez, H. Dulot, H. Gonzalez-penas, M. Courtiade, D. Thiebaut, *Abst. Pap. Am. Chem. Soc.* 236 (2008) 37-PETR.
- [24] T. Dutriez, M. Courtiade, D. Thiebaut, H. Dulot, F. Bertoncini, M.C. Hennion, *J. Sep. Sci.* 33 (2010) 1787.
- [25] T. Dutriez, M. Courtiade, D. Thiebaut, H. Dulot, F. Bertoncini, M.C. Hennion, *J. Chrom. A* (2010) In Press.
- [26] T. Dutriez, M. Courtiade, D. Thiebaut, H. Dulot, M.C. Hennion, *Fuel* 89 (2010) 2338.
- [27] T. Dutriez, M. Courtiade, D. Thiebaut, H. Dulot, J. Borrás, F. Bertoncini, M.C. Hennion, *Energy Fuels* 24 (2010) 4430.
- [28] L. Fang, S. Kulkarni, K. Alhooshani, A. Malik, *Anal. Chem.* 79 (2007) 9441.
- [29] D.W. Armstrong, T. Payagala, L.M. Sidisky, *LC-GC Eur.* 22 (2009) 459.
- [30] J.L. Anderson, D.W. Armstrong, *Anal. Chem.* 77 (2005) 6453.
- [31] T. Payagala, Y. Zhang, E. Wanigasekara, K. Huang, Z.S. Breitbach, P.S. Sharma, L.M. Sidisky, D.W. Armstrong, *Anal. Chem.* 81 (2008) 160.
- [32] J.V. Seeley, S.K. Seeley, E.K. Libby, Z.S. Breitbach, D.W. Armstrong, *Anal. Bioanal. Chem.* 390 (2008) 323.
- [33] V.R. Reid, J.A. Crank, D.W. Armstrong, R.E. Synovec, *J. Sep. Sci.* 31 (2008) 3429.
- [34] W.C. Siegler, J.A. Crank, D.W. Armstrong, R.E. Synovec, *J. Chromatogr. A* 1217 (2010) 3144.
- [35] R.E. Murphy, M.R. Schure, J.P. Foley, *Anal. Chem.* 70 (1998) 1585.
- [36] W. Khummueng, J. Harynuk, P.J. Marriott, *Anal. Chem.* 78 (2006) 4578.
- [37] J.T. Andersson, A.H. Hegazi, B. Roberz, *Anal. Bioanal. Chem.* 386 (2006) 891.
- [38] T. Schade, B. Roberz, J.T. Andersson, *Polycyclic Aromat. Compd.* 22 (2002) 311.
- [39] S.K. Panda, W. Schrader, J.T. Andersson, *J. Chromatogr. A* 1122 (2006) 88.
- [40] A.H. Hegazi, J.T. Andersson, *Energy Fuels* 21 (2007) 3375.
- [41] R. Ong, P. Marriott, P. Morrison, P. Haglund, *J. Chromatogr. A* 962 (2002) 135.
- [42] T.L. Chester, J.W. Coym, *J. Chromatogr. A* 1003 (2003) 101.
- [43] L. Ramos, *Comprehensive Two Dimensional Gas Chromatography*, Wilson & Wilson's, Madrid, 2009.
- [44] B. Omais, M. Courtiade, N. Charon, A. Quignard, D. Thiebaut, *J. Chromatogr. A* (2010) Submitted.
- [45] D.L. Massart, B.G.M. Vandeginste, L.M.C. Buydens, *Handbook of Chemometrics and Qualimetrics, Part A*, Elsevier, Amsterdam, 1997.
- [46] G. Derringer, R. Suich, *J. Qual. Technol.* 12 (1980) 214.
- [47] J. Vial, M. Cohen, P. Sassiati, D. Thiebaut, *Curr. Med. Res. Opin.* 24 (2008) 2019.
- [48] I.P. Fisher, P. Fischer, *Talanta* 21 (1974) 867.